

COVER PAGE

Document downloaded by @DAEL

Mon Nov 9 14:39:04 2026
For personal use

When automatic English translation is provided, only the original document is authentic.
The EAA cannot be held responsible of any translation error

Bibliographical reference

The Influence of the Horn Effect in Tyre/Road Noise, J. H. Schutte, Y. H. Wijnant and A. De Boer, Acta Acustica **vol. 101** (Number 4), 2015, pp. 690-700

DOI
https://doi.org/10.3813/AAA.918865

Acta Acustica united with Acustica
Vol. 101 (2015) 690 – 700

DOI 10.3813/AAA.918865

The Influence of the Horn Effect in Tyre/Road Noise

J. H. Schutte, Y. H. Wijnant, A. de Boer
University of Twenty, Faculty of Engineering Technology, P.O. Box 217, 7500 AE Enschede, The Netherlands.
j.h.schutte-1@alumnus.utwente.nl

Summary
The horn effect is known as an important amplification mechanism in tyre/road noise. The name is referring to the geometry between tyre and road surface which resembles an exponential horn. The horn effect is a common subject for both experimental and numerical research. Contrary to previous studies which considered point sources, this paper focusses on the horn effect by simulated tyre vibrations. The amplification of acoustic pressure, however, depends largely on the location of the observer. The sound power can be used as a measure for the horn effect which is independent on the point of observation. In this paper, the sound radiation problem is solved using the boundary element method (BEM). First, a case study considering equivalent point sources is used to validate the accuracy of the boundary element model and solver using experimental results. Next, the vibrations of tyres rolling on textured road surfaces are investigated numerically. The computed tyre vibrations are used to study the horn effect using different tyre designs. The amplification by horn effect is determined by the combined tyre/road geometry and the distribution of the noise. The current method may be used to systematically study the influence of the horn effect, for example, during tyre development.

PACS no. 43.20.-f, 43.40.-r, 43.50.-x

1. Introduction

In modern society, traffic noise has become an important issue for mental health. A significant contributor to this noise pollution is exterior tyre/road noise. Tyre/road noise, which is caused by the interaction between tyre and road surface, is dominant for almost all driving speeds. From experiments, it is known that spectra of tyre/road noise display a broad peak somewhere in the range of 500–2000 Hz [1]. Different structural and aerodynamical generation mechanisms have been identified, although the contribution of these mechanisms depend on the tyre, road, speed and other conditions.

Next to these generation mechanisms, amplification or reduction mechanisms are distinguished as they amplify or attenuate tyre/road noise. The so-called horn effect is considered as an important amplification mechanism [1]. At the leading and trailing edge, the air between the tyre and the road surface forms a shape which resembles an exponential horn. Due to the geometrical shape between tyre and road, the acoustic impedance changes gradually and sound radiation is efficient. The same phenomenon is used in musical instruments, for example. The effect is most pronounced for acoustic wavelengths, which are approximately equal to the radius of the tyre. The horn effect provides significant amplification of the noise sources, which are located in the tyre/road gap, of about 10–20 dB [2].

Kropp, Bécot, et al. [3, 4, 5] used a two-dimensional model to study the horn effect of a tyre above a reflecting surface. The initial multipole synthesis [5] has been replaced by an efficient method using equivalent sources [4]. It has been concluded that the horn effect is maximal at frequencies around 2 kHz in the plane of the tyre and its amplification can be reduced by an absorbing road surface. An increase in distance from the source to the reflecting plane resulted in lower amplification above 800 Hz [5]. Other studies on the horn effect are performed by, among others, Klein [6, 7], who applied the two-dimensional multipole synthesis. Two-dimensional models are numerically efficient, although they can only be used to qualitatively study the horn effect in the plane of the tyre. Graf, Kuo, et al. [2, 8] studied the horn effect experimentally and numerically. Besides the boundary element method (BEM) [2], they used ray theory for high frequencies and a scattering model for low frequencies [8]. The results show that wider tyres radiate sound more efficiently and that rounding the tyre edges can reduce the horn effect. Morgan and Watts used BEM to investigate the acoustic performance of shields and enclosures [9].

BEM is an appropriate method to investigate external noise radiation. Brick [10, 11] applied a half-space BEM method to tyres and investigated the contribution of the individual tyre modes to the overall sound radiation. A detailed tyre geometry is an important prerequisite for a cor-

Received 24 March 2014,
accepted 12 February 2015.

© S. Hirzel Verlag · EAA

Document downloaded by @DAEL, 2026-11-09 14:39:07 - personal use only

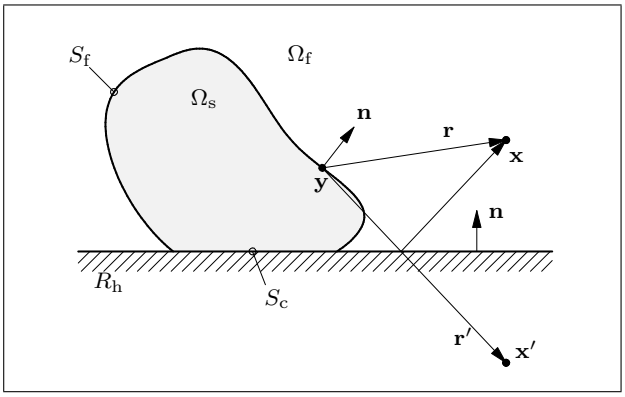


Figure 1. Overview and nomenclature of the baffled exterior acoustic problem. Source points **y** are positioned on the free boundary S_f of a closed cavity Ω_s. Partially the boundary S is in contact with an infinite baffle (S_c) with reflection coefficient R_h. The mirror field points $\mathbf{x}'$ contribute to **x**.

rect sound radiation model. More recently, Graham [12] used a reciprocal-configuration BEM calculation to study the influence of the geometric parameters on the radiation characteristics. Reducing the tyre width limits the amplification of noise sources on the tire belt. Jean et al. [13] used a mixed integral/ray tracing approach to study tyre/road noise. BEM is used to solve the sound radiation accurately close to the contact zone and beam tracing is employed outside this area. The applied strategy is a trade off between accuracy and simulation time.

Over the past decades, the horn effect has been the subject for both experimental and numerical research. Although numerical investigations have mainly focussed on point sources, tyre vibrations have been used for the simulation of the horn effect. Jean et al. [13] used results from a two dimensional plate model [14] in their sound radiation analysis. In order to describe the horn effect realistically, the horn effect should be calculated using tyre vibrations. These vibrations can be determined by a three-dimensional numerical tyre/road noise model [15, 16] and used in a sound radiation model using BEM.

This paper focusses to two new aspects regarding the horn effect. *Primarily*, the use of a three-dimensional numerical model to both calculate the tyre vibrations and study the horn effect is newly presented in this paper. Afterwards this complete model can be used for a parametric study of the tyre pattern with respect to the horn effect. *Secondary*, the use of sound power to quantify the horn effect. In literature the amplification is usually evaluated at single points. Since the horn effect depends largely on the location of the observer, it makes sense to compare sound power levels rather than local sound pressure levels, as will be presented in this paper. An elaborate study using sound power levels is unknown to the authors.

The outline of this paper is as follows. In section 2, the basic theory and implementation of sound radiation are presented. The numerical model consists of a boundary element model which is discussed in section 3 and a source model which is discussed in section 4. The results for two different source models are discussed in section 5. Finally, conclusions are drawn and possibilities for future research are given in section 6.

2. Sound radiation

In this section, the basic theory and the numerical implementation of sound radiation are discussed. The application will be discussed in the subsequent sections. The theory of exterior sound radiation is presented for the general case of a vibrating object on a (partially) reflective baffle, i.e. a tyre on a road surface. It is assumed that the vibrations are harmonic and that sound radiation can be solved in the frequency domain using linear acoustics. The numerical problem is solved using the boundary element method (BEM).

2.1. Theory

The theory on linear acoustics is frequently described in literature and therefore discussed briefly only; for an overview the reader is referred to, for example, [17, 18]. Consider a vibrating object Ω_s above an infinite baffle with reflection coefficient R_h, presented in Figure 1. The object is radiating sound to an external fluid medium Ω_f. In the boundary element method, the acoustic wave equation needs to be described on the boundary surface. Green's second identity can be used to define the *Helmholtz integral equation* (HIE), which for no incident pressure wave, reads

$$\alpha(\mathbf{x})p(\mathbf{x}) = \oint_S \left(\frac{\partial G_\mathrm{h}(r)}{\partial n} p(\mathbf{y}) + \mathrm{i}\omega\rho_0 G_\mathrm{h}(r) v_n \right) \mathrm{d}S. \qquad (1)$$

where $\alpha(\mathbf{x})$ is the space angle in a field point **x**, $p(\mathbf{x})$ is the acoustic pressure in a field point, $G_\mathrm{h}(r)$ denotes Green's half-space function, r is the distance between source and field point, **n** is the normal vector on the surface, $p(\mathbf{y})$ is pressure on the source ($\mathbf{y} \in S$), ω represents the angular frequency, ρ_0 is the undisturbed density, v_n is the normal velocity of the source and S is the boundary. The coefficient α is zero in the solid domain i.e. tyre ($\mathbf{x} \in \Omega_\mathrm{s}$), unity in the fluid domain i.e. air ($\mathbf{x} \in \Omega_\mathrm{f}$) and $0 \leq \alpha \leq 1$ on the boundary ($\mathbf{x} \in S$). The boundary surface S consists of a free part S_f and a part in contact S_c.

2.2. Implementation

In the *direct boundary element method*, the boundary integral formulation in equation 1 is evaluated. First, the acoustic variables on the boundary surface are solved using a collocation scheme. After substituting appropriate shape functions and rewriting, the following system of equations is obtained [18],

$$\mathbf{p}_\mathrm{s} = \mathbf{H}_\mathrm{ss} \cdot \mathbf{v}_n. \qquad (2)$$

$\mathbf{H}_\mathrm{ss}$ denotes the global transfer matrix between surface velocities $\mathbf{v}_n$ and source pressures $\mathbf{p}_\mathrm{s}$ on the surface. Equation 2 is commonly referred to as the Surface Helmholtz

Document downloaded by @DAEL, 2026-11-09 14:39:07 - personal use only

Integral Equation Formulation (SHIEF). The pressure in the field $\mathbf{p}_f$ can be calculated using the source pressures $\mathbf{p}_s$ or directly using a different global transfer matrix $\mathbf{H}_{fs}$.

$$\mathbf{p}_f = \mathbf{H}_{fs} \cdot \mathbf{v}_n. \tag{3}$$

Equations 2 and 3 are solved by the boundary element solver BEMSYS, developed by Visser [18].

Schenck [19] introduced interior constraints to remove the non-uniqueness of the Helmholtz integral equation which resulted in the Combined Helmholtz Integral Equation Formulation (CHIEF). Later on, improvements to the CHIEF method have been made by, e.g. Wu and Seybert [20]. In addition to the CHIEF method, Burton and Miller [21] proposed an integral equation that is valid for all wave numbers. The Burton-Miller approach solved the non-uniqueness problem, although suffers from singular integrals in the derivative equation. The algorithm used in this work is the Combined Interior Burton-Miller Formulation (CIBFM) [18], a combination of the ordinary SHIEF method with the interior Burton-Miller approach. The CIBFM preserves the accuracy and convergence behaviour and guarantees uniqueness throughout the full frequency range.

The solver in BEMSYS is different from other solvers in the way the numerical integration is applied. Green's kernel is split into a singular and oscillatory part in order to solve both parts in different ways. The singular or wave number independent part is solved by *standard* Gauss-Legendre quadrature, while the oscillatory or wave number dependent part is solved by *adaptive* Gauss-Legendre quadrature. Therefore, the solver can be applied to study small gaps accurately, as will be discussed in Section 3. The uniqueness, accuracy and convergence of the solver have been validated with experimental and numerical examples. For more information about the solution procedure and validation of BEMSYS the reader is referred to [18].

3. Boundary element model

In this section the boundary element model of a tyre on a reflective road surface will be discussed. The vibrational source is discussed in the subsequent section. BEM requires a closed radiating surface, referred to as *source mesh*. The deformed tyre shape will be used as a basis for the source mesh, see (1a) in Figure 2. The source mesh can be more refined near the contact zone. In order to obtain a closed mesh, the gaps at the rims will be covered, see (1b) in Figure 2. On these rim meshes the normal velocity is zero for all frequencies. The combined source mesh consists of bilinear quadrilateral elements, as depicted in Figure 2. The element size is important for the accuracy of the numerical model. As a rule of thumb, at least six elements are required per wavelength [22]. For the current mesh, this 'six elements per wavelength rule' is satisfied up to 2.75 kHz and up to 2.5 kHz in case of tyre vibrations. At higher frequencies the accuracy of the solution decreases.

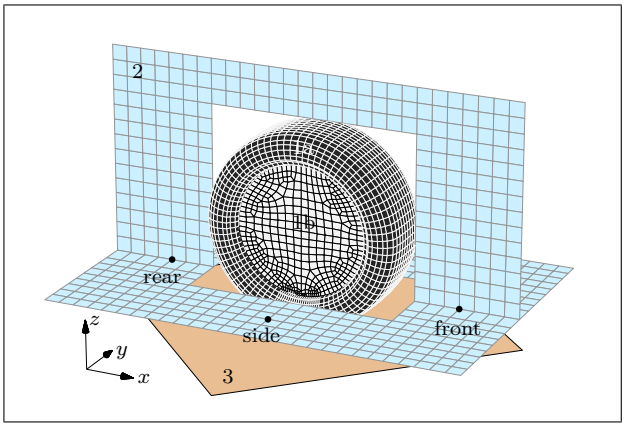


Figure 2. Source mesh of tyre (1a+1b) and field mesh (2) on a reflective baffle (3); the evaluation positions are marked by a (•).

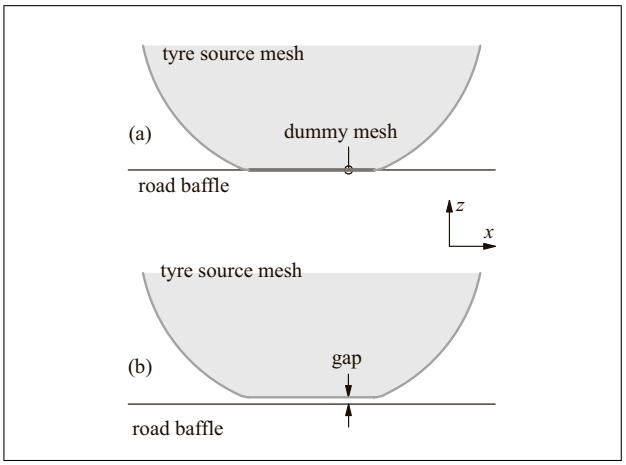


Figure 3. Contact between tyre source mesh and road baffle: dummy contact mesh (a) and small gap (b).

In BEMSYS, in order to solve the Helmholtz integral equation, a set of constraint points is defined on a fictitious surface inside the actual boundary surface. The points are determined automatically using the boundary element mesh. An adaptive mesh refinement algorithm is used to improve the solution of the singular parts of the integrals. For more information the reader is referred to Visser [18].

The road is modelled as a flat plane of infinite dimensions, generally referred to as a *baffle* [17]. The texture of the road is not taken into account in the radiation model. Acoustical absorption can be taken into account in the sound radiation model [15]. For equivalent point sources, however, the baffle is assumed to be acoustically hard. This implies total reflection without a phase shift, i.e. the reflection coefficient $R_h = 1$.

The contact area between the tyre and the road can be modelled in two ways, see Figure 3. In the first approach, the part of the source mesh which intersects with the baffle is separated from the source mesh and treated separately as a dummy mesh. On this so-called *dummy contact mesh* the velocities are set to zero. In the second approach, a *small gap* can be taken into account between the source mesh and the baffle. In order to prevent discrepancies, this gap

Document downloaded by @DAEL, 2026-11-09 14:39:07 - personal use only

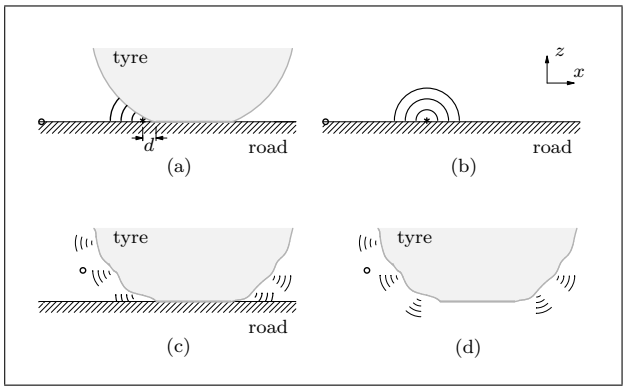


Figure 4. Two methods to study the horn effect: (I) the SPL ratio at a receiver (∘) due to an equivalent point source (∗) while the tyre is present (a) to the case where the tyre is omitted (b); (II) the SPL ratio at a receiver (∘) due to a vibrating tyre with (c) and without (d) a road baffle.

has to be much smaller than the shortest wavelength (highest frequency) in the model. A distance between tyre and impedance plane has been used in [11] as well. The choice for the most appropriate method depends on the vibrations of the tyre, as will be discussed in the next section.

By a post-processing step the acoustic pressure is calculated in nodes around the tyre. These nodes can be connected in a *field mesh*, which is used for visualization purposes only. The standard field mesh consists of two planes: (i) a horizontal plane through the so-called CPX (Close Proximity Measurement) positions (0.1 m above the road) and (ii) a vertical symmetry plane. In order to obtain a rectangular mesh, elements close to the tyre source mesh are discarded, as given in Figure 2. Extra field points can be added at any exterior point around the tyre.

4. Source model

In the previous sections the theory and implementation of the boundary element model has been discussed. A description of the source model has not been presented yet. There are two ways to investigate the horn effect. The first approach considers point sources which are placed close to the horn of the tyre. The second approach takes vibrations of the tyre surface into account.

4.1. Equivalent point source

In the classical approach, a point source is put on the reflective baffle, close to the centre of the horn, see figures 4(a-b). The influence of the presence of the tyre and road is calculated afterwards. In literature there is no unique definition of the horn effect available. The most frequently used definition of the horn effect reads

$$\Delta\mathrm{SPL} = 20\log_{10}\left|\frac{p_{\mathrm{tr}}(\mathbf{x})}{p_{\mathrm{r}}(\mathbf{x})}\right| = \mathrm{SPL}_{\mathrm{tr}} - \mathrm{SPL}_{\mathrm{r}}, \qquad (4)$$

where $p_{\mathrm{tr}}(\mathbf{x})$ denotes the pressure at field points in presence of the tyre and road and $p_{\mathrm{r}}(\mathbf{x})$ the pressure at field points in absence of the tyre (i.e. road only). The horn effect can be interpreted as the SPL difference in a certain configuration, see Figure 4(a), with respect to a reference configuration, see Figure 4(b). This classical method to determine the horn effect will be referred to as method I.

The observed amplification due to the horn effect depends greatly on the location of the field point. The sound power W may be used to define an alternative ratio which does not depend on the location of the observer. The sound power equals

$$W = \frac{1}{2}\Re\oint_S p(\mathbf{y})\,\overline{v_n}(\mathbf{y})\,\mathrm{d}S, \qquad (5)$$

where $\Re$ denotes the real part and $\overline{v_n}$ is the complex conjugate of the normal velocity. The horn effect can be expressed alternatively as the ratio of the radiated sound power with and without the tyre ΔSWL,

$$\Delta\mathrm{SWL} = 10\log_{10}\left(\frac{W_{\mathrm{tr}}}{W_{\mathrm{r}}}\right) = \mathrm{SWL}_{\mathrm{tr}} - \mathrm{SWL}_{\mathrm{r}}, \qquad (6)$$

where W_{tr} denotes the sound power including tyre and road and W_{r} represents the sound power in absence of the tyre.

In order to be consistent with presented studies in literature, a dummy contact mesh will be used for the equivalent point sources study. The utilization of a dummy contact mesh, however, does not have a significant influence. This will be validated in section 5.1.

4.2. Tyre vibrations

In order to study the horn effect more realistically, simulated tyre vibrations can be used as noise source rather than equivalent point sources. The vibrations of a tyre rolling on a textured road surface are calculated according to Schutte [15, 16] and afterwards used as boundary conditions for the sound radiation analysis. The numerical simulation of tyre/road noise is performed by means of three subsequent models. For completeness the models are only discussed briefly, for more information the reader is referred to [15, 16].

4.2.1. Tyre vibration model

First the tyre cross-section is virtually mounted to the rim and inflated in a two-dimensional analysis. In this step, stresses due to the internal pressure are taken into account. Next, a three-dimensional tyre geometry is generated and the results from the first step are used as an initial condition for this model. Then, a steady-state rolling calculation is performed in which inertia effects (centrifugal forces) are taken into account. In the final step, the transient rolling tyre is modelled using the Lagrangian approach. The tyre mesh needs to be sufficiently refined in order to capture tyre/road interaction. An explicit scheme is used to solve the resulting large system of equations.

A standard but highly-refined finite element model of the tyre has been developed in Abaqus containing about 1 million degrees of freedom. Slick tyre models have been

Document downloaded by @DAEL, 2026-11-09 14:39:07 - personal use only

discussed in literature before, e.g. see [23]. The tyre mesh consists of three-dimensional solid elements including so-called rebar layers to model the reinforcement layers. Rubber material is modelled using hyperelastic models to capture the non-linear, isotropic material behaviour. A time-domain viscoelastic material model has been modelled using Prony series.

The road is modelled as a rigid non-smooth surface. A road surface consists of a dense texture spectrum which should be taken into account in a numerical simulation. Constructing a synthetic road surface requires measurement scanning data at a high spatial resolution. These data were not available. Using an alternative method, a rectangular texture map is generated from randomly distributed white noise. The road surface is flattened (the tops of the texture are removed) and filtered (interpolation is used to make the surface more smooth) in order to mimic a 'real' road surface. Along several lines the final road surface has been validated in the spatial frequency domain using measurement results [24].

The tyre/road contact problem is defined as a pure master/slave configuration in Abaqus, where the rigid road is the master and the deformable tyre is the slave (hard contact definition). In normal direction, the kinematic contact algorithm is used to solve contact using a predictor/corrector algorithm. In tangential direction, a standard Coulomb friction model has been assumed.

4.2.2. Coupling

In a second model, the resulting vibrations of the tyre surface are interpolated from a rotating to a fixed mesh and transformed to the frequency domain. A one-way coupling between the vibration model and sound radiation model is assumed, i.e. the normal velocities are assumed not to depend on the acoustic pressure. For an acoustic radiation problem, the mesh can be coarser compared to an equivalent structural vibration problem. Nevertheless, it is possible to apply local mesh refinement close to the contact zone.

4.2.3. Sound radiation model

Finally, the tyre vibrations are then used as boundary conditions in a sound radiation model. The model includes a three-dimensional boundary element model of a tyre above a reflecting baffle. Tyre/road noise is calculated in the frequency domain. This boundary element model has been discussed in detail in section 3.

In case of tyre vibrations, the description of the contact between tyre and road becomes important in the sound radiation model. The use of a dummy mesh has two major disadvantages. First, it is hard to determine which nodes of the fixed mesh are in contact, since nodes on the rotating finite element mesh are moving in and out of contact. Second, vibrations are discarded because nodes in the contact zone can have a normal velocity, specifically when tyres are running on coarse road surfaces. Therefore, a small gap between the tyre and road is assumed.

Physically, the gap can be justified since the tyre is rolling on top of the road texture peaks [5]. It is advantageous that no dummy contact mesh is needed and that no information is lost. The adaptive integration makes BEMSYS suitable for small gaps and thin geometries [18].

Since the tyre has to be present as vibration source, an alternative definition of horn effect is proposed,

$$\Delta\mathrm{SPL} = 20\log_{10}\left|\frac{p_{\mathrm{baffled}}(\mathbf{x})}{p_{\mathrm{free}}(\mathbf{x})}\right|, \tag{7}$$

where $p_{\mathrm{baffled}}(\mathbf{x})$ is the acoustic pressure in a field point $\mathbf{x}$ for baffled tyre situation and $p_{\mathrm{free}}(\mathbf{x})$ is the acoustic pressure in case of a free vibrating tyre (road is omitted). This method will be referred to as method II. In graphical representation, the baffled configuration given in Figure 4(c) is compared to a reference configuration in Figure 4(d). A sound power ratio can be defined accordingly as

$$\Delta\mathrm{SWL} = 10\log_{10}\left(\frac{W_{\mathrm{baffled}}}{W_{\mathrm{free}}}\right), \tag{8}$$

where W_{baffled} and W_{free} denote the sound power for a baffled and a free situation, respectively.

5. Results

5.1. Equivalent point source

The main objective of this case study is to validate the boundary element model using BEMSYS. Visser [18] has investigated the horn effect in BEMSYS already for a coarse cylindrical geometry. This case study considers a detailed tyre geometry and an experimental validation with experimental results by Kropp et al. [10, 5].

In the numerical model, a 175 SR14 tyre is scaled in width to 220 mm and pressed onto a flat road surface under normal loading conditions, see Figure 5. The obtained *deformed* tyre geometry is used in the present analysis; the undeformed tyre radius is 318 mm. The contact width is around 130 mm, where the border of the contact area is denoted as the origin of the horn. The equivalent point source (∗) is approximated by a normal velocity of a single node on the tyre surface. The source location is located at $d = 80$ mm of the origin of the horn in the wheel centre plane[1], see Figure 5. The influence of the horn is analyzed at a field point at 1 m distance from the horn's centre (•). The road surface is modelled as an infinite fully reflective baffle. The field mesh is shown in Figure 5, displaying the sound pressure at $f = 1334$ Hz.

In Figure 6 the amplification due to the horn is given for the field point at 1 m distance. The numerical model is in very good agreement with the experimental results. The horn effect is responsible for amplifications up to 14 dB over a wide frequency band around 1 kHz. The location

[1] The tyre or wheel centre plane is the xz-plane through the centre of the rim axis.

Document downloaded by @DAEL, 2026-11-09 14:39:07 - personal use only

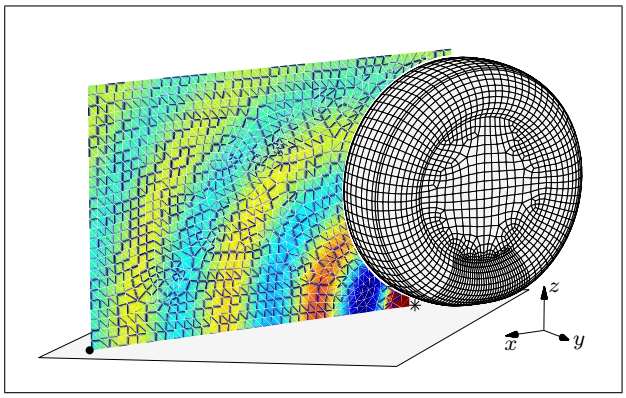


Figure 5. Configuration of the tyre positioned on a fully reflective baffle with point source (∗) and field point (•). The field mesh shows the real part of the pressure at $f = 1334$ Hz.

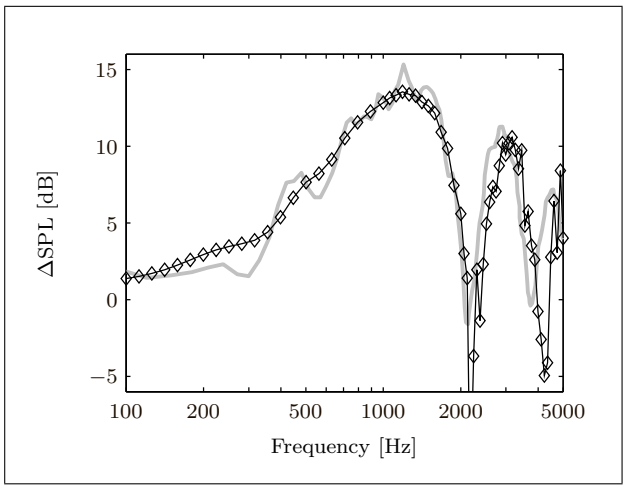


Figure 6. Sound pressure difference ΔSPL for a tyre on a rigid plane (source point at 80 mm and field point at 1 m distance): numerical model (◇) and experimental data (grey line) from [5].

and height of the peak is dependent on the distance between the source and the border of the contact patch d, the width of the tyre, and the field point considered. The amplification is known to be most pronounced in the wheel centre plane (xz-plane). At some frequencies the presence of the tyre is reducing the radiated sound in the studied field point, e.g. at 2.18 kHz. These narrow frequency bands depend on the location of the source and field point. Due to the size of the tyre, the influence of the horn is only limited for frequencies below 500 Hz. Maximum amplification is observed when the wavelength is approximately equal to the tyre radius.

The difference in sound power level ΔSWL does *not depend* on the location of the field point, see Figure 7. The frequency of the peak appears at roughly the same frequency as ΔSPL in Figure 6. The height of the peak, however, is lower since the highest amplification is observed in the wheel centre plane. At very low frequencies ($f < 150$ Hz) the horn effect is slightly counterproductive, i.e. SWL is reduced. At high frequencies, the horn effect decreases to zero.

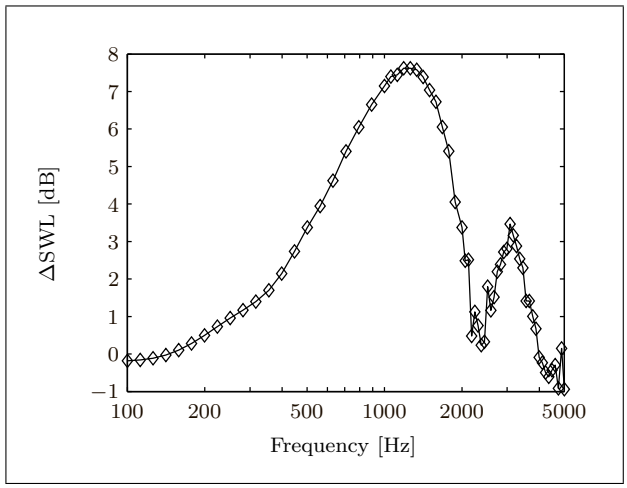


Figure 7. Sound power difference ΔSWL for an equivalent point source at 80 mm.

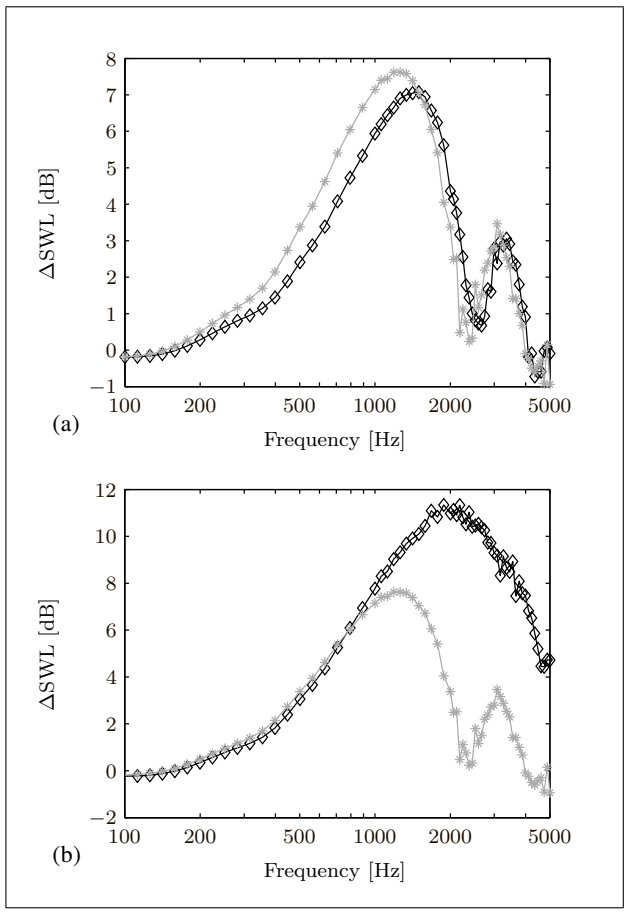


Figure 8. Sound power difference ΔSWL as a function of tyre width and source location. (a) Tyre width: 175 mm (◇) and 220 mm (∗), (b) Source location: 36 mm (◇) and 80 mm (∗). (a) Tyre width: 175 mm (◇) and 220 mm (∗), (b) Source location: 36 mm (◇) and 80 mm (∗).

In Figure 8, ΔSWL is presented due to changes in width of the tyre and changes in source location. Wider tyres, in general, lead to a slightly higher amplification peak and a frequency shift towards lower frequencies, see Figure 8(a). The results are in accordance with [2, 12]. When the noise

Document downloaded by @DAEL, 2026-11-09 14:39:07 - personal use only

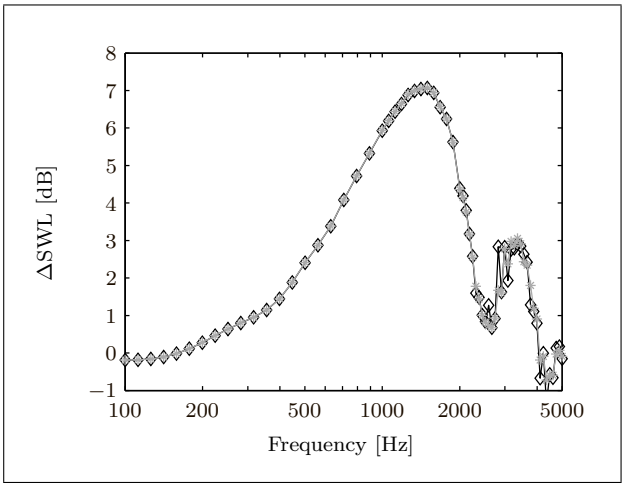


Figure 9. Sound power difference ΔSWL with (∗) and without (◇) a dummy contact mesh (source location: 80 mm, tyre width: 175 mm).

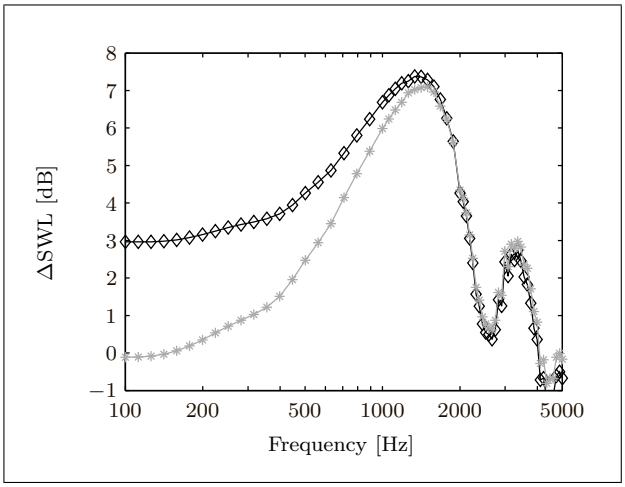


Figure 10. Sound power difference ΔSWL according to method II (◇) equation 8 and method I (∗) equation 6 (source location: 80 mm, tyre width: 175 mm).

source is moved from 80 mm towards 36 mm from the horn's centre, the total sound power is more than doubled, see Figure 8(b). Moving the source even closer to the origin of the horn leads ultimately to a limit amplification [2, 5]. It can be concluded that the tyre vibrations close to the contact zone are efficiently radiated into the far field. A realistic velocity distribution is therefore important. The influence of the horn effect on simulated tyre vibrations will be studied in section 5.2.

Before we discuss the results of the tyre vibration simulation, the influence of a dummy contact mesh and the definition of the horn effect are studied. In the study considering equivalent point sources, by default, a dummy contact mesh has been used. Instead of using a dummy contact mesh, the source mesh can be extended and the road surface baffle can be shifted down by a very small distance with respect to the smallest wavelength. In Figure 9, ΔSWL is shown for a simulation with and without a dummy contact surface for a point source at 80 mm. For frequencies below 3 kHz, the differences between both methods are hardly noticeable.

In Figure 4, the two definitions of the horn effect, i.e. method I and II, are compared. In the equivalent point sources study, the influence of the presence of the tyre (method I) has been studied already. It is also possible to study the influence of presence of the road (method II), which will be used to study the tyre vibrations. In Figure 10, ΔSWL is presented for both methods, as calculated using equations 6 (method I) and 8. For low frequencies, method II predicts a 3 dB larger SPL values than method I. In this low frequency region, the tyre is small with respect to the wavelength and sound waves will simply pass the tyre. The sound power is distributed in all directions, instead of just one half-plane, as is the case when a point source is put close to an infinite baffle. For higher frequencies, the curvature of the tyre becomes negligible and the tyre resembles an infinite baffle. Both methods converge to the same solution. It can be concluded that the boundary element model is appropriate to study the horn effect quantitatively.

Table I. Settings for horn effect study.

Description	Value	Unit
tyre vibration model		
number of circumferential elements in tyre mesh	200	
inflation pressure	2.3	bar
tyre radius	323	mm
static loading pressure	4810	N
rolling speed	80	km/h
source model		
number of source points	2882	
frequency step	10	Hz
reflection coefficient road baffle	0.1	

5.2. Tyre vibrations

In this section we consider two 235/45 R17 tyres rolling on synthetic ISO 10844 asphalt, i.e. a smooth road surface, at a speed of 80 km/h: (i) a slick tyre and (ii) a longitudinally grooved tyre. Some basic settings for the tyre vibration model are presented in Table I.

The grooved tyre shares the construction with the slick tyre, but contains three, symmetrically positioned longitudinal grooves. Each undeformed groove has a width of 10 mm and a depth of 8 mm. Note that the groove will deform in and close to the contact region. A longitudinally grooved tyre can be considered as the time-averaged geometry of a patterned tyre as well. At certain frequencies f, the grooves can act as a so-called $\lambda/2$ resonator [25],

$$f = \frac{nc}{2(L + 0.8d)}, \tag{9}$$

where n is an integer number, c is the speed of sound, L the groove length and d the diameter of the groove. For the

Document downloaded by @DAEL, 2026-11-09 14:39:07 - personal use only

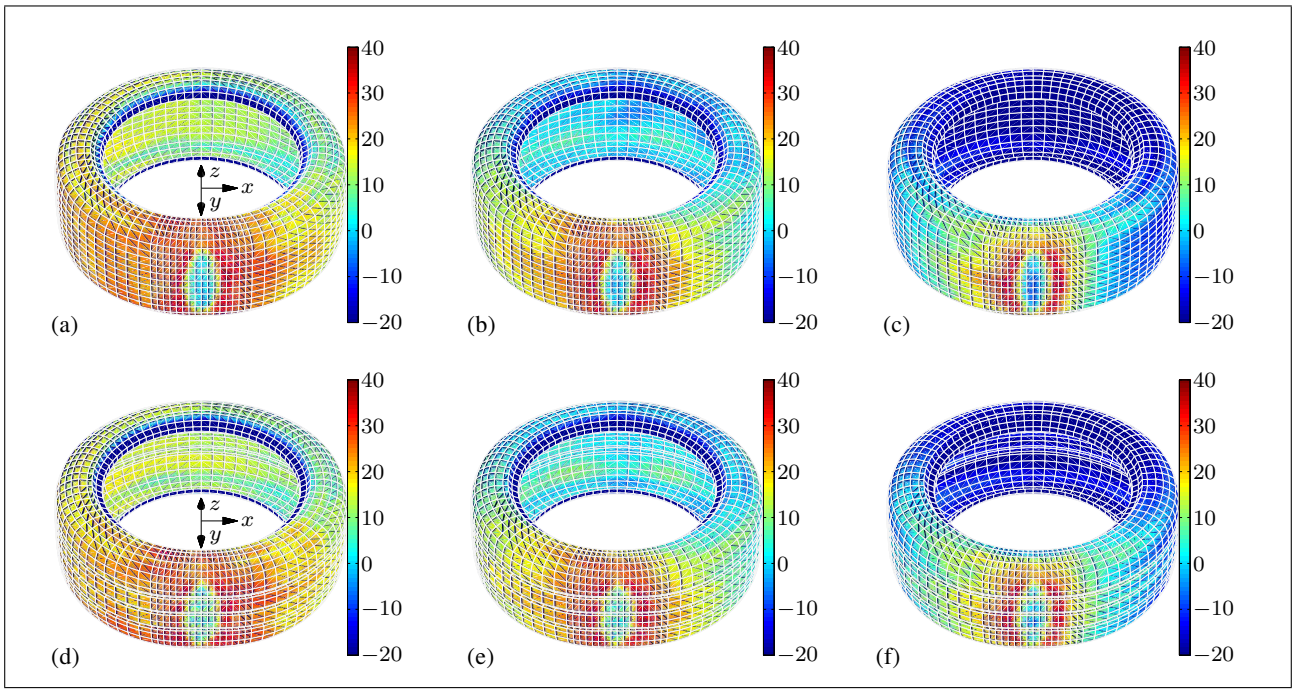


Figure 11. Absolute normal velocity $|v_n|$ in 1/3 octave bands [dB re 1 mm/s] on the slick tyre (a–c) and grooved tyre (d–f) surface (the tyres are rolling in the positive x-direction). (a,d) $f = 500$ Hz, (b,e) $f = 1000$ Hz, (c,f) $f = 2000$ Hz.

longitudinally grooved tyre ($L \simeq 0.1\,m$ and $d \simeq 9\,mm$), the *first* resonance frequency of the groove is around 1.6 kHz.

Since the excitations of both tyres rolling on an ISO 10844 surface are calculated separately, the tyre vibrations and distribution over the surface differ as well. The small absorption ($\alpha = 0.1$) of the road surface baffle reduces the amplification slightly at high frequencies, see Table I. In the subsequent figures, the levels are presented in 1/3 octave bands in order to smooth the results within a certain frequency band. The computed excitations are generally complex and differ for each frequency step. The spread in amplification for the individual frequency steps is actually quite high, as will be discussed using Figure 14.

In Figure 11 the absolute normal velocities $|v_n|$ are presented in 1/3 octave bands [dB re 1 mm/s] for three different frequencies on the slick and the longitudinally grooved tyre surface. All tyres are rolling in the positive x-direction. Note that the results are mapped on the fixed source mesh, which is more refined around the contact zone. The largest vibrations are found close to the contact surface; in the contact surface itself the vibrations are very small. At 500 Hz the tyre vibrations spread along the full tyre surface, while at 2 kHz the vibrations remain close to the contact zone. The differences in vibration pattern between a longitudinally grooved tyre and a slick tyre are small.

Figure 12 shows the amplification by the horn effect ΔSPL in 1/3 octave bands for three different frequencies around the slick and the longitudinally grooved tyre. The directivity for different frequency bands is nicely illustrated. The horn effect is most effective for high frequencies at the wheel centre plane (xz-plane). Towards the sides and above the tyre, the horn effect is less important. So, the observed amplification depends largely on the position of the observer. Moreover, the figures illustrate that the amplification increases with the frequency. The differences between the slick and the grooved tyre are most pronounced for the higher frequencies. The grooved tyre shows a larger ΔSPL at 1 and 2 kHz compared to the slick. A possible reason is the increased radiation surface of a grooved tyre. Contrary to the slick tyre, vibrations of the groove bottom can radiate efficiently to far-field, even in the contact area. Hence, the influence of amplification of longitudinal pipe resonances is taken into account.

Figure 13 shows the sound pressure level difference ΔSPL as function of the frequency at three positions close to the tyre, as marked in Figure 2. In general, ΔSPL is larger at the front and rear side of the tyre compared to the sides. The smaller differences between front and rear side can be explained by the slight tyre deformation due to rolling. The difference in ΔSPL between the two tyres is clearly visible. The horn effect is more pronounced for the longitudinally grooved tyre since the grooves contribute as well. The influence of the grooves is more pronounced for the higher frequencies. The horn effect for tyre vibrations is somewhat different from the horn effect by equivalent point sources, compare figures 6 and 13. In case of tyre vibrations, all nodes on the surface are vibrating randomly. The nodes close to the contact zone have the highest velocity. For excitation sources close to contact, the amplification shifts towards higher frequencies. This observation is in accordance with the case study considering point sources. Hence, also the absorption of road surfaces such as porous asphalt concrete is most efficient in the 1–2 kHz frequency region. The sound power level SWL will be used to compare different configurations.

Document downloaded by @DAEL, 2026-11-09 14:39:07 - personal use only

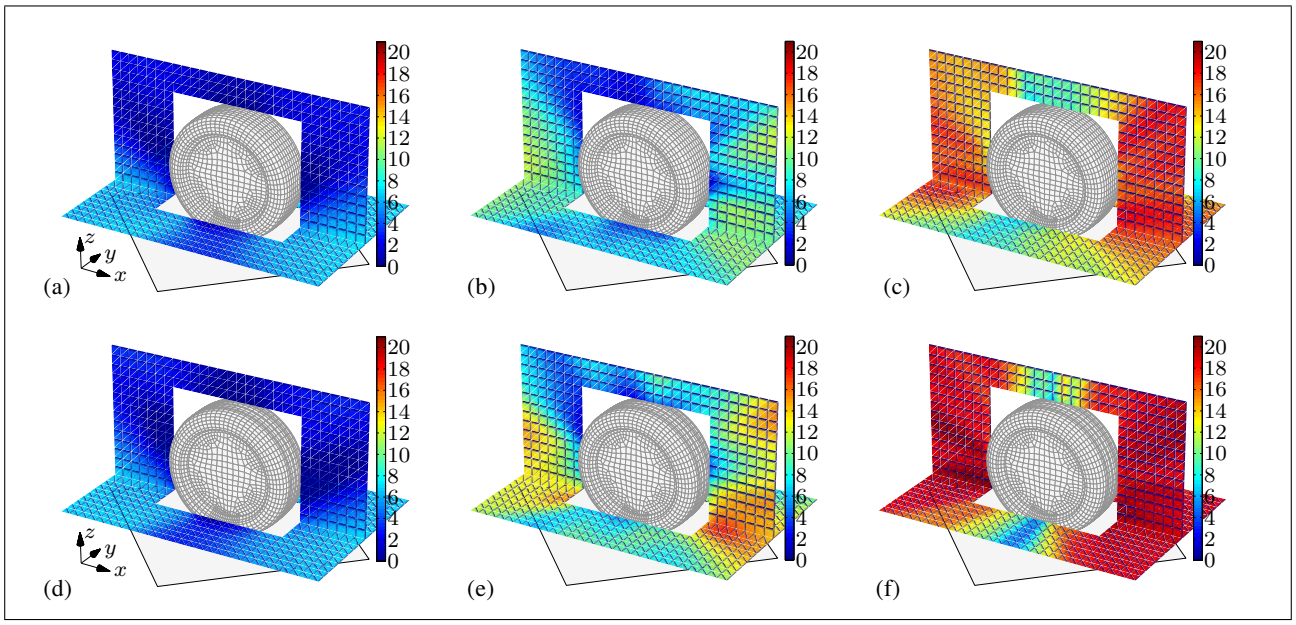


Figure 12. ΔSPL [dB] in 1/3 octave bands [dB re $2 \cdot 10^{-5}$ Pa] at a field around the slick tyre (a–c) and grooved tyre (d–f) (the tyres are rolling in the positive x-direction). (a,d) $f = 500$ Hz, (b,e) $f = 1000$ Hz, (c,f) $f = 2000$ Hz.

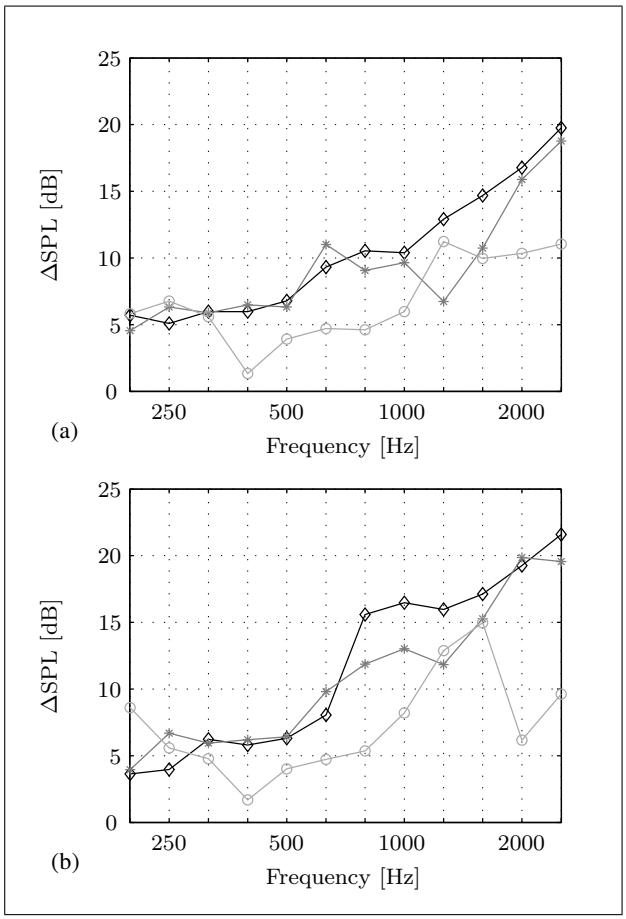


Figure 13. Sound pressure difference ΔSPL in 1/3 octave bands for tyres rolling on ISO 10844 at 80 km/h at different positions: front (◇), rear (∗) and side (○). (a) Slick tyre, (b) Longitudinal grooved tyre.

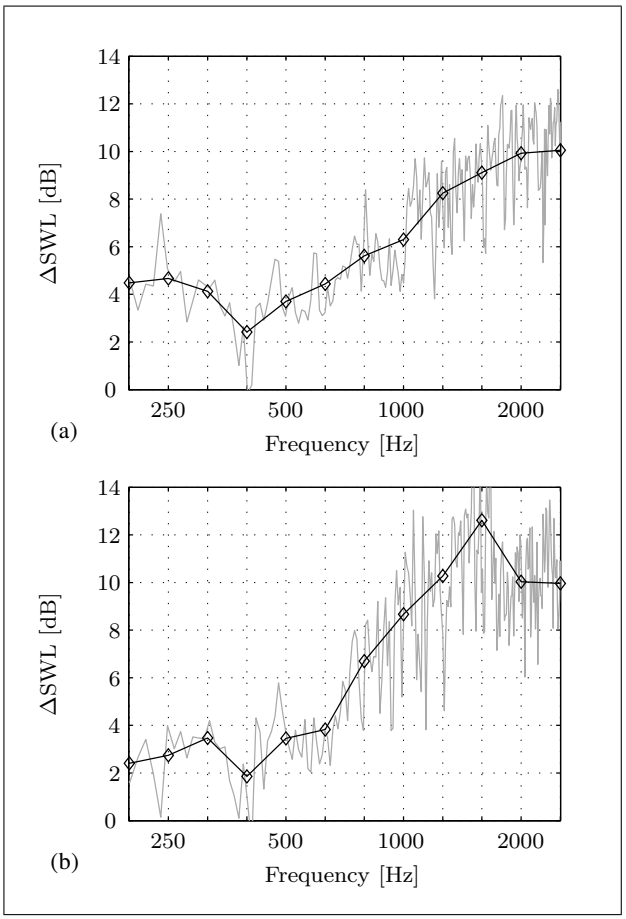


Figure 14. ΔSWL [dB] in 1/3 octave bands for tyres rolling on ISO 10844 at 80 km/h (the gray line shows the computed values). (a) Slick tyre, (b) Longitudinally grooved tyre.

Document downloaded by @DAEL, 2026-11-09 14:39:07 - personal use only

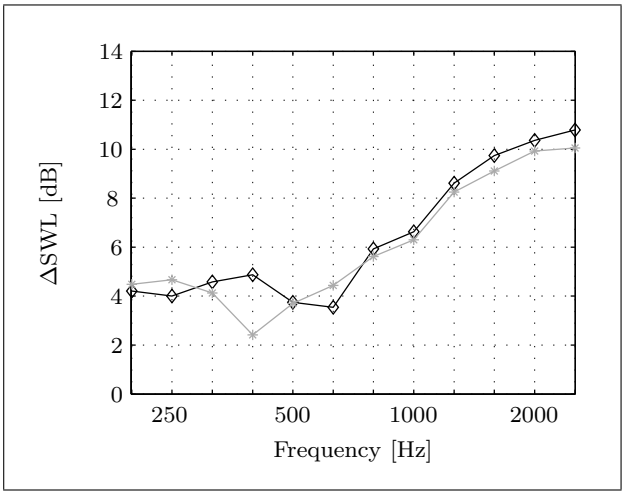


Figure 15. ΔSWL [dB] in 1/3 octave bands for a slick tyre rolling at 80 km/h on SMA 0/16 (◇) ISO 10844 asphalt (∗).

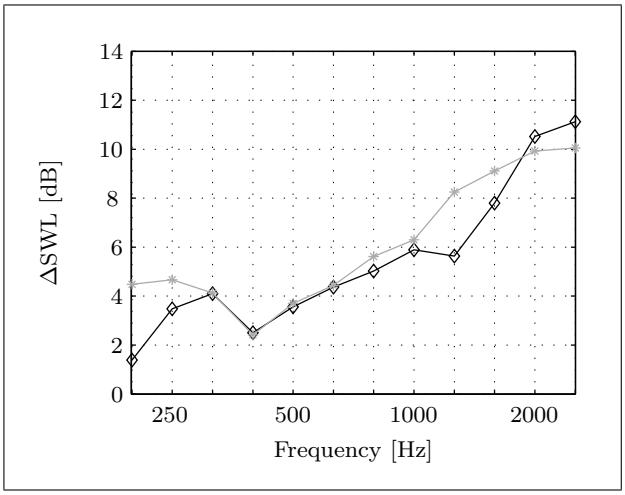


Figure 16. ΔSWL [dB] in 1/3 octave bands for a slick tyre with thin (◇) and thick (∗) tread rubber rolling at 80 km/h on ISO 10844 asphalt.

Figure 14 shows the sound power level difference ΔSWL for the slick and the grooved tyre. Since the computed values have a large spread, the values are averaged using 1/3 octave band filter. Note that the horn effect has been evaluated using method II, which results in a 3 dB increase in ΔSWL at low frequencies compared to method I. That explains why ΔSWL is minimal at 400 Hz and increases slightly for lower frequencies. For higher frequencies, ΔSWL increases to a maximum value of 10 dB for a slick and 12.5 dB for a grooved tyre. This is in accordance with the increase in SPL. The difference between slick and grooved tyre is the most pronounced at the pipe resonance frequency of 1.6 kHz.

5.2.1. Numerical study

The horn effect can be studied systematically using the same strategy as presented in this paper. In a short numerical study, we will investigate the influence of the road and the tyre structure.

In the previous analysis, we considered axisymmetric tyres rolling on a smooth ISO 10844 road surface. When a slick tyre is rolling on a coarser road surface, such as stone mastic asphalt (SMA) 0/16, the sound pressures and sound power change significantly. The horn effect, on the other hand, changes marginally, see Figure 15. This can be explained by the minor changes in the mean tyre shape, contact area and vibration distribution across the tyre surface. The mean tyre shape and the distribution of vibrations determine the amplification by the horn effect. For extremely coarse road surfaces, the tyre will roll on top of the texture peaks only. The horn geometry, i.e. tyre shape and distance from tyre to reflection plane, will change and therefore the observed amplification. The effect of increasing the distance from source to reflection plane has been investigated by [5].

In a second study, a slick tyre with a reduced tread thickness is considered. The tyre has the same construction as the reference slick, is cured in the same mould and is inflated to the same pressure, however it has a reduced tyre stiffness. Note that the radii of the tyre shoulders are changing as a result of the thinner tread. The shoulder radius does influence the radiation efficiency [11, 12]. The results are compared in Figure 16. The differences between both slick tyres are marginal. The changed tyre geometry leads to a decrease in ΔSWL around 1.25 kHz and an increase around 2.5 kHz. Nevertheless, the tyre stiffness can be used to influence the amplification over the frequency bands.

6. Conclusions

The horn effect has been studied numerically using both sound pressure levels and sound power levels. Contrary to the sound pressure level, the sound power level is not dependent on the location of the observer. The traditional approach to determine the horn effect, i.e. by placing point sources close to the horn shape between tyre and road, confirmed the accuracy of the used sound radiation model. In a new approach, the horn effect has been studied by considering simulated tyre vibrations as the excitation source. Mainly at frequencies above 1 kHz, the horn effect is an important amplification mechanism. The numerical simulations showed that the tyre vibrations are the largest close to the contact zone. Moreover, these vibrations contribute most to the sound radiated to the far-field at high frequencies. The amount of amplification depends on the combined tyre/road geometry and the distribution of the sources i.e. tyre vibrations. As long as the contact patch and the distribution of the tyre vibrations do not change much, the influence of the road is limited. This is the case for smooth asphalt road surfaces. The road, however, becomes important when its texture is very coarse and the tyre is rolling on the peaks of the surface. From the tyre point of view, longitudinal pipe resonances are amplified by the horn geometry. The vibrating groove walls can radiate efficiently, even in the contact zone, because the impedance is matched to the free field.

Document downloaded by @DAEL, 2026-11-09 14:39:07 - personal use only

The current study can be used to investigate the horn effect systematically. It may be possible decrease influence of the horn, although the possibilities are limited. Neither the tyre nor the road can be removed and slick tyres are not road legal. One may think of geometrical changes, since the horn effect depends largely on geometry. The tyre design can be changed by, for example, decreasing the tyre width, optimizing the lateral grooves and rounding the tyre shoulders. The tyre's radial stiffness, amongst others, determines the size of the contact zone. On the other hand, sound absorbing road surfaces can be applied. Mainly at high frequencies sound absorption of road surfaces is very effective. Finally, the path of the acoustic waves from source to observer can be changed. The car body work and the wheel arches can be optimized, and a shielding or enclosure around the tyre can be applied.

Acknowledgments

The support of TNO and Apollo Vredestein B.V. within this CCAR project is gratefully acknowledged by the authors.

References

[1] U. Sandberg, J.A. Ejsmont: Tyre/road noise reference book. First ed. INFORMEX, Harg, SE-59040 Kisa, Sweden, 2002.

[2] R.A.G. Graf, C.-Y. Kuo, A.P. Dowling, W.R. Graham: On the horn effect of a tyre/road interface, part I: Experiment and computation. Journal of Sound and Vibration **256** (2002) 417–431.

[3] F.-X. Bécot, W. Kropp: Iterative equivalent sources model of the tyre emission over impedance surfaces. Proceedings of the 5th European Conference on Noise Control, Naples, Italy, 2003.

[4] F.-X. Bécot, P.J. Thorsson, W. Kropp: An efficient application of equivalent sources to noise propagation over inhomogeneous ground. Acta Acustica united with Acustica **88** (2002) 853–860.

[5] W. Kropp, F.-X. Bécot, S. Barrelet: On the sound radiation from tyres. Acustica **86** (2000) 769–779.

[6] P. Klein: Horn effect characterisation for tire-road noise radiation. Proceedings of Inter-noise 2000, Nice, France, 2000.

[7] P. Klein: Tyre noise horn effect on an absorbing road surface – 2D analytical modelling using the multipole synthesis. Proceedings of Inter-noise 2002, Dearborn, Michigan, USA, 2002.

[8] C.-Y. Kuo, R.A.G. Graf, A.P. Dowling, W.R. Graham: On the horn effect of a tyre/road interface, part II: Asymptotic theories. Journal of Sound and Vibration **256** (2002) 433–445.

[9] P.A. Morgan, G.R. Watts: A new approach for evaluating the sound propagation from a moving vehicle tyre using boundary element methods. Tech. Rept. TRL Published Project Report, PPR137, TRL Limited, 2006.

[10] H. Brick, M. Ochmann, W. Kropp: Point-source-scattering from tyre-like structures above an impedance plane. Proceedings of NAG/DAGA 2009, Rotterdam, The Netherlands, 2009.

[11] H. Brick: Application of the boundary element method to combustion noise and half-space problems. Dissertation. Chalmers University of Technology, Sweden, 2009.

[12] W.R. Graham: Influence of tire geometry on the horn effect. Proceedings of Inter-noise 2012, New York City, USA, 2012.

[13] P. Jean, N. Noe, F. Gaudaire: Calculation of tyre noise radiation with a mixed approach. Acta Acustica united with Acustica **94** (2008) 91–103.

[14] W. Kropp: Ein Modell zur Beschreibung des Rollgeräusches eines unprofilierten Gürtelreifens auf rauher Strassenoberfläche. Dissertation. Institut für Technische Akustik, Berlin, Germany, 1992.

[15] J.H. Schutte: Numerical simulation of tyre/road noise. Dissertation. University of Twente, Enschede, The Netherlands, 2011.

[16] J.H. Schutte, E. Verhulp, Y.H. Wijnant, A. de Boer: Simulation of tyre/road noise by means of a FEM/BEM approach. European Congress on Computational Methods in Applied Sciences and Engineering (ECCOMAS 2012), Vienna, Austria, 2012, J. Eberhardsteiner, H. Böhm, F. Rammerstorfer (eds.), Vienna University of Technology, 1–10.

[17] R.D. Ciskowski, C.A. Brebbia: Boundary element methods in acoustics. Computational Mechanics, Southampton, 1991.

[18] R. Visser: A boundary element approach to acoustic radiation and source identification. Dissertation. University of Twente, Enschede, The Netherlands, 2004.

[19] H.A. Schenck: Improved integral formulation for acoustic radiation problems. J. Acoust. Soc. Am. **44** (1968) 41–58.

[20] T.W. Wu, A.F. Seybert: A weighted residual formulation for the chief method in acoustics. Journal of Sound and Vibration **90** (1990) 1608–1614.

[21] A.J. Burton, G.F. Miller: The application of integral equation methods to the numerical solution of some exterior boundary-value problems. Proceedings of the Royal Society of London. Series A, Mathematical and Physical Sciences, 1971.

[22] S. Marburg, B. Nolte (eds.): Computational acoustics of noise propagation in fluids – Finite and boundary element methods. Springer-Verlag Berlin Heidelberg, 2008.

[23] M. Brinkmeier, U. Nackenhorst, S. Petersen, O. von Estorff: A finite element approach for the simulation of tire rolling noise. Journal of Sound and Vibration **309** (2008) 20–39.

[24] W. Schwanen, H.M. van Leeuwen, A.A.A. Peeters, G.J. van Blokland, H.F. Reinink, W. Kropp: Acoustic Optimization Tool: RE3: Measurement data Kloosterzande test track. Tech. Rept. M+P.DWW.06.04.8, M+P – consulting engineers, 2007.

[25] U. Sandberg: Tyre/road noise – Myths and realities. Proceedings of Inter-noise 2001, The Hague, The Netherlands, 2001.

Document downloaded by @DAEL, 2026-11-09 14:39:07 - personal use only